Amplified radiative cooling via optimised combinations of aperture geometry and spectral emittance profiles of surfaces and the atmosphere

G.B. Smith,
Physics and Advanced Materials, University of Technology, Sydney, PO Box 123
Broadway NSW 2007, Australia
Email g.smith@uts.edu.au
Fax +61 2 95142219 Ph +61 2 95142224

Abstract

Net thermal radiation cooling, from surfaces at sub-ambient temperatures, to the night sky is amplified if the aperture to the sky is partially blocked with heat mirrors. The temperature at which radiation loss stagnates (the effective sky temperature) falls continuously as the aperture closes and is derived in terms of the aperture size and the spectral properties and temperatures of the atmosphere and of the emitting surface. Cooling surfaces must have high absorptance between 7.9 μm to 13 μm where the atmosphere is most transparent. The best response for the remainder of the Planck radiation spectrum surprisingly switches between two spectral extremes at a temperature which falls as the aperture gets smaller. A perfect absorber is best above this switch, while surfaces which reflect all of this radiation are best below it. A simple formula is presented for the cross-over temperature as a function of aperture size. With known material properties plus representative non-radiative heat gains a high emittance surface is generally better except when heat mirrors are not used. A known high emittance roof paint at 10° C below ambient, under a 45° aperture lined with shiny aluminium, can achieve a net output power near 135 Wm^{-2} under a clear sky.

Keywords : radiative cooling, sky, atmosphere, apertures, selective surfaces, emittance

1.Introduction

Adaptation to global warming will substantially raise the demand for space cooling and refrigeration, while the need for large CO_2 emission reductions means cooling technologies need to become very much more energy efficient. It is also preferable to cool at night and store cold for the next day for better air conditioner COP's and to avoid large daytime demand peaks and overloaded grids. A major natural resource, the clear night sky, is available and underutilised, either for stand-alone heat pumping or use in hybrid systems with conventional cooling systems. Pumping heat at useful and substantial rates from surfaces whose temperature T_s is below ambient is possible because the atmosphere is partially transparent to thermal radiation, mainly over the limited band for wavelength λ between 7.9 μm to 13 μm within the Planck radiation spectrum $P(\lambda,T_a)$ at atmospheric temperature T_a. We label this band the "sky window". The atmosphere is largely opaque or "black" outside this band. It is also necessary to account for the continuous drop in transparency across this sky window for ray directions at angles η to the vertical which are increasingly further from the zenith[1]. Thus $e_a(\eta,\lambda)$, which defines the direction and wavelength dependence of atmospheric thermal emittance, is central to our analysis.

A key aspect of cooling technologies based on exploitation of the sky window is the spectral properties of the coating/substrate system defined by their spectral emittance $e_s(\eta,\lambda)$. Many practical coatings of interest emit uniformly, that is they are nearly Lambertian, so we will drop the η dependence in numerical examples for simplicity. In passing however it is worth noting that an alternative approach to the mirror based angular selectivity in this paper could be coating based via controlling the η dependence of $e_s(\eta,\lambda)$ using anisotropic nanostructures. There are two spectral extremes, which practical surfaces can approach. Both emit strongly across the sky window, which is essential for good sky cooling. However across the remainder of

the Planck radiation spectrum one absorbs 100% of incoming radiation and the other reflects 100% as shown in figure 1. The former is thus a “black body” and the latter an “ideal” spectrally selective sky radiator because it does not absorb any of the incident radiation from the atmosphere apart from the much reduced amount coming in within the sky window. Various approaches to near “ideal” radiators have been explored [2-4] and various composites or double layers can get quite close to the “ideal” in figure 1. The best compounds and layers on low emittance substrates for IR absorption confined mainly to the range 7.9 μm to 13 μm identified to date rely on narrow band ionic motion in lighter molecular weight materials containing two or more of Si, N, O, Al, Mg and C. Their substrate must have high IR reflectance and is typically vacuum coated [2-4], though painting may be feasible in some cases with suitable binders. Select gases also emit mainly in the right range [5]. Associated studies have been mainly limited to surfaces fully open to the sky hemisphere, which turns out in the analysis following to be where such “ideal” sky window spectral selectivity is preferable for typical operating temperatures. If however we seek to improve cooling rates by blocking some of the incoming radiation from the atmosphere at higher angles to the zenith then, as we will now show, the preferred spectral properties depend on T_s and the aperture. Most interestingly for operation at fixed T_s the optimum switches at a particular value of $(T_a - T_s)$ between these two extremes, rather than moving between them. This has clear engineering implications. There has been little work reported on night sky cooling within heat mirror apertures since the work many years ago by Trombe [6].

2. Models for heat mirror aperture dependence of radiant heat pumping

Blocking is done by confining the aperture to the sky to a limited solid angle, which we centre around the zenith in this analysis, but in some cases a tilt of the axis from the vertical may be advantageous. The simplest form is a truncated conical aperture with maximum zenith angle η_{max} . $\eta_{max} = \pi/2$ for a fully open surface. The generic conclusions using this model carry over to other aperture shapes with minor quantitative shifts. The structure used to create the aperture must have an internal

surface which is a good heat mirror, for example it could be aluminium. These mirrors must be specular to ensure no radiation is scattered back to the emitter, while their shape must also ensure no radiation is returned. This set up ensures that any incident radiation from directions closer to the horizontal is very much less than that from these directions in the atmosphere. Further remarks on practical heat mirror options, which in some cases resemble solar concentrators, follow later. To establish the principles here we first take them to be perfect reflectors to eliminate any radiation from them altogether. Another interesting option is to have the blocker surface itself quite cold. Suitable gases in special enclosures around the surfaces will keep these colder than ambient and can add to cooling both doing this and in some cases also through their own emissions.

Equation (1) gives the instantaneous net radiated power for an aperture with a conical opening to zenith angle η_{max} and perfect heat mirrors,

$$P_{rad} = \left[\int_0^{\pi/2} d(\sin^2\eta) \int_0^{\infty} d\lambda P(\lambda, T_s) e_s(\eta, \lambda) \right] - \left[\int_0^{\eta_{max}} d(\sin^2\eta) \int_0^{\infty} d\lambda P(\lambda, T_a) e_a(\eta, \lambda) e_s(\eta, \lambda) \right] \quad (1)$$

with the second term the energy absorbed from the atmosphere since $e_s(\eta,\lambda) = a_s(\eta,\lambda)$ the surface spectral absorptance. All outgoing radiation (the first term) escapes. With $e_s(\eta,\lambda) = 1$ or $e_s(\eta,\lambda) = 0$ for all directions it is independent of η and λ for both the black body, and also for the "ideal" sky emitter apart from it's step change at 7.9 μm and 13 μm. Thus equation (1) simplifies for the black body to equation (2a) and for the "ideal" sky window emitter to equation (2b).

$$P_{rad}^{BB} = \sigma T_s^4 - \sigma T_a^4 \left\{ \sin^2 \eta_{\max} [1 - \rho_{sw}(T_a)] + I_{sw}(\eta_{\max}) \rho_{sw}(T_a) \right\} \quad (2a)$$

$$P_{rad}^{ideal} = \left(\sigma T_s^4\right) \rho_{sw}(T_s) - \left(\sigma T_a^4\right) I_{sw}(\eta_{\max}) \rho_{sw}(T_a) \quad (2b)$$

with σ the Stefan Boltzmann constant. $\rho_{sw}(T)$ is the fraction of total energy under the Planck spectrum at temperature T within the range 7.9 μm to 13 μm and $I_{sw}(\eta_{max})$ is the definite integral of equation (3). It is an aperture factor which defines the total energy emitted by the atmosphere within the sky window range into any aperture, relative to what it would be with no aperture and a black or opaque atmospheric "sky window". As seen in equation (2a) or (3) with e = 1, for wavelengths where the atmosphere is opaque this aperture factor becomes $I_{BB}(\eta_{max}) = \sin^2(\eta_{max})$.

$$I_{sw}(\eta_{\max}) = \int_0^{\eta_{\max}} d(\sin^2 \eta) e_{a,sw}(\eta) \qquad (3)$$

In equation (3) we have replaced $e_a(\eta,\lambda)$ within the sky window by its spectral average $e_{a,sw}(\eta)$ at each zenith angle η. $e_a(\eta,\lambda) = 1$ outside this range. This is the approximate "box" model utilised by Likushu et. al. [5] for clear skies. It gives quite good estimates of practical net radiative cooling powers with $e_{a,sw}(\eta) \approx 1 - 0.87^{1/\cos\eta}$. Using this model the build up of incoming energy as the aperture opens, as determined by $I_{BB}(\eta_{max})$ and $I_{sw}(\eta_{max})$, for both segments of the Planck spectrum are compared in figure 2. The factor $\rho_{sw}(T)$ varies slowly with temperature T and is in the range 0.28 to 0.32 at the temperatures of most practical interest in night sky cooling. Equation (2b) tells us immediately that standard emittance e_s, which is the weighted average of $e_s(\lambda)$ over the full Planck spectrum for the "ideal" emitter, is $\rho_{sw}(T)$. Standard emittance data for practical sky window emitters is a useful quick quality check, with the better ones typically having e_s in the range 0.30 to 0.35.

Both equations (2a) and (2b), and indeed all practical radiators, can be recast in the well known generic form of equation (4) except that the temperature defining the average hemispherical surrounds is no longer T_a but an effective sky temperature T_a*, which depends on both the aperture solid angle as defined by η_{max}, and the spectral properties of the emitting surface. T_a* is also obviously the temperature at which radiative loss stagnates. At any lower T_s there would be a net radiative gain from the atmosphere.

$$P_{rad} = e_s \sigma \left[T_s^4 - \left(T_a^* \right)^4 \right] \quad (4)$$

For the ideal emitter as a Lambertian surface $e_s = \rho_{sw}(T_s)$, and for the black body $e_s = 1.0$. T_a* is defined for each of these extremes using equations (2a) and (2b) to be respectively,

$$T_{a,BB}{}^*(\eta_{\max}) = T_a \left\{ \sin^2 \eta_{\max} \left[1 - \rho_{sw}(T_a) \right] + I_{sw}(\eta_{\max}) \rho_{sw}(T_a) \right\}^{1/4} \quad (5a)$$

$$T_{a,ideal}{}^*(\eta_{\max}) = T_a \left[I_{sw}(\eta_{\max}) \rho_{sw}(T_a) \right]^{1/4} \quad (5b)$$

with use of the approximation $\rho_{sw}(T_s) = \rho_{sw}(T_a)$. It is easy to modify 5(b) to account for differences in these two numbers when T_s and T_a are far apart. Other inputs (see later) usually prevent cooling to T_a* but it is still very useful to know its value. We focus on T_s down to around 20° below ambient. With attention to thermal design and maybe lower values of η_{max}, even with corrections for non-ideality and other heat gains, it may be feasible to achieve even lower temperatures overnight. Trombe [6] achieved 30 °C to 40 °C below ambient in similar set ups. For an aperture of 5° with T_a = 17°C , T_a* is -193° C or 200 °C below ambient for the black body, and 229 °C below for the "ideal" surface. Interestingly for small apertures the black body surface is preferable at all practical temperatures, while for intermediate apertures cross-over becomes an issue as seen in figure 3. Plots of net heat pumping by radiation as a function of T_s at various fixed T_a are easily generated from equations (2) and (3) or (4) and for the 45° aperture and the open surface are plotted in figure 3. On the axis where $T_a = T_s$ two additional points are plotted for a 45 ° aperture with known practical surfaces which approach these two ideals. For the near black body we took $e_s = a_s = 0.95$ and for the near ideal surface we take absorptance $a_s = 0.90$ between 7.9 μm and 13 μm and $a_s = 0.1$ outside the sky window range. Other aspects of practical systems detailed in section 4 following have been included in these two points apart from non-radiative gains, which are absent when $T_a = T_s$.

3. The cross-over temperature from high emittance to "ideal" emitter

Table 1 provides a comparison for T_a = 290°K (17°C), of net radiant powers for $T_s = T_a$ and when T_s is 10 °C and 20 °C below ambient, for a fully open surface and a conical aperture of 45°. Two other features of interest are included in this table which vary with aperture size (a) radiation stagnation temperature or T_a* (b) the approximation to cross-over temperature T_{sx} given in equation (6). Above T_{sx} the black body surface provides superior cooling powers, while below T_{sx} the ideal surface pumps out more net radiant heat. It is also obvious by extrapolation of the two lowest curves that the black body emitter is always much superior for above ambient temperatures. T_{sx} is the solution of T_s when equations (2a) and (2b) are equated and since $\rho_{sw}(T)$ varies slowly with T a useful estimate for how far T_{sx} is below ambient becomes

$$T_a - T_{sx} = T_a \left[1 - \sqrt{\sin \eta_{\max}}\right] \qquad (6)$$

For cross-overs more than 25° C below ambient T_{sx} is seen in figure 3 to be slightly lower than the approximation of equation (6) since then variations in $\rho_{sw}(T)$ with T do have an impact, but such errors have marginal significance given the proximity of performance near cross-over .

The amplification of the black body output going from an open panel to one seeing only 45° of sky is much larger than that for the ideal sky emitter surface. The absolute values of heat pumped per unit area of emitting surface with this aperture means that at temperatures to which useful heat pumping is likely to occur and that appear achievable a near black body will be superior to all other set ups. Working temperatures overnight will depend on many factors including, sky conditions especially humidity, starting or input temperatures, thermal mass to be cooled, thermal insulation, heat exchanger design, and flow rates if applicable. In addition the various departures from ideality we discuss in the next sections must be accounted for. Ongoing studies will fill in this information but initial indications are that with 45° or smaller aperture heat mirrors, heat pumping down

to 15°C below ambient looks achievable but ~30°C below ambient may be possible in some circumstances.

The gain with the ideal emitter in using the aperture relative to no aperture is seen in figure 3 to be marginal down to 30° C below ambient. Thus this type of spectrally selective surface appeals most for use when radiative blocking is absent or small. However with intermediate apertures and actual materials which approach this surface spectrally, they may have a role at very low temperatures, say more than 25° below T_a, which might be useful in a tandem system in which the high emittance surface comes first.

4. Practical radiators and structures

The impressive pumping rates in table 1 represent physical limits and will not be achieved in practice, but they form a good basis for realistic estimates of the potential of this technology, as well as insights into key design principles. Given the large differences in output from the two surfaces well away from cross-over as in figure 3, the relative merits of intermediate spectral properties are worth a mention. A surface or emitter approaching one or other of the two extremes is to be preferred, but an intermediate spectral character with high absorptance extending into the non-sky window range will be superior to ideal sky window emitters whenever the black body is best. This occurs in practice also when there is some blocking and T_s is within 20° C of ambient. It is interesting in this regard to note that use of a moderate density of CO_2 gas within a heat mirror lined aperture improves performance noticeably [6] while the same pressure of argon gave no additional cooling. CO_2 has quite high absorption beyond the sky window range to around 18 μm but larger partial pressures would be needed to add to absorption in the sky window range. It also helps cool the mirrors. Some cooling tasks involve a wide range of temperatures so if this range spanned T_{sx} an intermediate spectral property might be preferred.

Experimental surfaces of interest relative to the two limiting spectral emittance plots in figure 1, have peak absorptance values in the rage 0.90 to 0.95. Among those which have high absorptance and hence near black body emittance ~0.95 across the whole Planck range, select ones including some special white paints, have excellent solar reflectance as well, which is an additional advantage . We have found this leads to an early start of net cooling in the afternoon. These surfaces being "white" at solar energy wavelengths and "black" at thermal wavelengths, are spectral opposites of the best selective surfaces for solar thermal technology. We have found that on a roof their night cooling impact adds significantly to performance [7]. Use on 35,000 square metres of Melbourne airport roof [8] has led to CO_2 emission reductions above 4,000 tonnes in 18 months. From equation (4) the reduction factor for radiant output is given directly by e_s which is 0.95 for this special paint.

The peak absorptance value in known near "ideal" sky window emitters can reach around 0.90 so that their absorptance a_s in the sky window becomes $a_s \sim 0.90$. They also have a correction for finite values of absorptance (~ 0.1) outside the range 7.9 μm to 13 μm. Then $e_s = 0.9\rho_{sw}(T_s) + 0.1[1 - \rho_{sw}(T_s)] = 0.34$. Down to $T_a - 20°$ the 0.1 term adds to output and input by small, slightly different amounts, so it is a reasonable approximation to neglect it, though we include both contributions in table 2 below for completeness.

IR transparent covers such as polyethylene to reduce convection are important to consider, though some aperture structures can reduce convection inputs naturally. Covers also help to limit and even eliminate the impact of dew formation. If present they reduce both output and input, which leads to a reduction factor for net output power near 0.90 if covers are thick enough for desired rigidity.

The impact of non-ideality of the heat mirrors is easily estimated from an additional integral in equation (1) to cover the zenith aperture angles η_{max} to $\pi/2$ with a constant low emittance value e_{mirror} for the metal mirrors in place of the

atmospheric emittance. The resulting addition to incoming radiation with the mirrors at $T = T_a$ is given by

$$\Delta P_{mirror} = (\sigma T_a^{\,4}) e_{mirror} \cos^2 \eta_{\max} \qquad (7)$$

so for $\eta_{max} = 45°$ and $e_{mirror} = 0.1$ the net reduction in output due to the heat mirrors being not perfect is $0.05(\sigma T_a^{\,4})$ which is 10% of the input from the atmosphere in the range 0° to 45°. The key point is without this mirror the extra atmospheric radiation input at zenith range 45° to 90° would double that from 0° to 45° (i.e. a factor 10 times what the mirror radiates). The factors noted so far are weakly temperature dependent and their combined impact on net loss for the black body and the ideal emitter leads to the practical system estimates plotted in figure 3 on the output power axis P when $T_s = T_a$. Estimates of the values for each contribution discussed so far can be found in table 2. Their use in both figure 3 and at the end of table 2 assumes they do not change significantly by 10°C below ambient.

Once $(T_a - T_s) > 0$ non-radiative temperature dependent heat gains from the local environment by conduction and convection across the difference $(T_a - T_s)$ reduce net output. They may become the dominant correction at surface temperatures more than 10 °C below ambient in simple structures. This term depends on thermal design and the aperture structures when used. We take as a good guide a non-radiative U value around 1.5 $Wm^{-2}\,°C^{-1}$. A full account on this issue is best done in the context of particular experimental studies.

The estimates of individual corrections to the ideal values in table 1 and their combined net impact on power output at 10°C below an ambient of 17°C are listed in table 2 for the 45° aperture case. With no aperture the values in table 1 and figure 3 are corrected by the same factors but leaving out the mirror term. Estimates are to the nearest 5 Wm^{-2}. At 45° apertures for surfaces approaching the "ideal", *total output* drops by 45 Wm^{-2} to yield a net rate of 55 Wm^{-2}, while with no heat mirrors

their *net total* heat pumping rate at 10° C below ambient is also close to 50 Wm^{-2}. Thus as with the perfect "ideal" surface, closing the aperture has little value at these temperatures for the "nearly ideal" surface. For the high e_s surfaces in contrast, for example the paints noted above, practical net heat output values are still enhanced by a large factor under an aperture. At a 45° aperture to the zenith their correction from table 2 is larger at 65 Wm^{-2} but *net total heat output* remains exceptionally attractive at 135 Wm^{-2}. For no aperture however this surface with $e_s = 0.95$ has a much lower net output near 15 Wm^{-2} at 10° C below ambient. This is under half of that for known "near ideal" surfaces in the same arrangement. Thus the estimated gain in *total* output power in using a 45° aperture and with $e_s \sim 0.95$ is around a factor of 8 relative to a surface with no heat mirror blocking, and a factor of 3 relative to either configuration of the near ideal sky window spectral system. If however radiant blocking by heat mirrors is not used the near ideal sky window system becomes superior at 10° C below ambient, by a factor ~3 relative to the surface with $e_s \sim 0.95$. Practical stagnation temperatures at which total cooling ceases are actually lower for the high emittance surface within the 45° aperture than the near ideal emitter, unless values of non-radiative U below 1.0 Wm^{-2} are achieved.

Radiative blocking structures might be considered by analogy to solar concentrators to be costly, to be unaesthetic, and to use a larger area overall than the cooling surface. This doesn't have to be the case. The word "concentrator" is not really appropriate here. A better phrase considering the physics, is atmospheric radiation "blocker". Rigorous optics is not essential, and even simple vertical grid structures are useful. They can achieve around a 45° aperture with thin Al walls which do not waste much cooling area relative to the fully open surface. Thin Al walls also limit inwards conduction, but such blockers must stand above the surface by an insulating gap. If the thin grid walls were Al coated plastic low heat gains ensue more easily. Their cell structures also limit convection gains.

There is scope for improvements to each factor used in the practical performance estimates given table 2, especially with additional attention to thermal design, but cost

may then become an issue. The estimates used are based around what we perceive to be low cost systems, implemented using known materials.

5. Conclusion

With attention to the interplay between the spectral properties of cooling surfaces, the average temperatures at which cooling is desired, and the use or otherwise of apertures in which the inner surfaces act as heat mirrors, very attractive values of net heat pumping by radiative cooling to the night sky are possible. For many expected applications a moderate aperture along with a high emittance output surface will give by far the superior sub-ambient output relative to all other design choices with up to 135 Wm^{-2} expected in practice at 10°C below ambient. These concepts are not costly to implement with specially chosen paints often ideal, and have much to offer in cost effective adaptation to climate change without excessive use of electric power, and to overall emission reductions. It is time radiative night sky cooling received the wider attention its potential impact merits. It also has much potential for water collection and distillation [9].

Acknowledgements Angus Gentle, Geoff McCredie and Alex Revel for useful discussions, and help with initial relevant trials. Rex Lehmann for collaboration on high solar reflectance, high thermal emittance paints. This work is being supported by an ARC Discovery Grant DP0987354.

References

[1] M. Martin, P. Berdahl, Summary of results from the spectral and angular sky radiation measurement program, Solar Energy 33 (1984) 241-252.

[2] T.S. Eriksson, A. Hjortsberg, C.G. Granqvist, Solar absorptance and thermal emittance of Al_2O_3 films on Al: a theoretical treatment. Solar Energy Mat. 6 (1982) 191-199.

[3] M. Tazawa, H. Kakiuchida, G. Xu, P. Jin, H. Arwin, Optical constants of vacuum evaporated SiO film and an application, J. Electroceram. 16 (2006) 511-515.

[4] T.S. Eriksson and C.G. Granqvist, Infra red optical properties of silicon oxynitride films: experimental data and theoretical considerations, J.Appl. Phys. 60 (1986) 2081 - 2091.

5. E.M. Lushiku, A. Hjortsberg, C.G., Granqvist, Radiative cooling with selectively infra red emitting ammonia gas, J. Appl. Phys. 53 (1982) 5526-5530.

6. F. Trombe, Perspectives sur l'utilisation des rayonnements solaires et terrestres dans certaines régions du monde, Rev. Generale de Thermique, 6 (1967) 1285-1314.

7. J.M. Bell, G.B.Smith, R. Lehmann, Advanced Roof Coatings: Materials and Applications, Proc. Smart and Sustainable Built Environment (CD) (Paper T606), SASBE 2003, Brisbane, Australia, Nov 2003.

8. S. Davidson, SkyCool : an extraordinary paint on a hot tin roof, ECOS 119 (2004) page 12. (this paint exemplifies an overall spectral ideal for combining near black body radiative cooling and solar control) also see www.enviro.aero/MelbourneAirportandSkyCool.aspx

9. T.M.J Nilsson, G.A. Niklasson, and C.G. Granqvist, A solar reflecting material for radiative cooling applications : ZnS pigmented polyethylene, Solar Energy Mat. and Solar Cells 28, 175-193 (1992).

Figure and table captions

Figure 1. Spectral emittance - absorptance of the black body and ideal sky window emitter relative to the Planck radiation spectrum $P(\lambda,T_a)$ from an atmosphere at 290°K.

Figure 2. Comparison of the $I(\eta_{max})$ factors, or aperture dependent reductions in incoming power from the atmosphere, into a given conical aperture with a vertical axis, for wavelengths into which it radiates like a black body and those in the range 7.9 μm to 13 μm. All are relative to a fully open black body hemisphere.

Figure 3. Net radiative cooling powers from the two limiting surfaces, black body and ideal sky emitter, for a conical aperture of 45° and a fully open surface. The two points on the axis marked with triangles are estimates of where materials approximating these two surfaces inside real 45° mirror set-ups might start. Radiative cooling curves emanating from these points will be near parallel to those plotted at 45°.

Table 1 Comparison of net radiative cooling powers at $T_s = T_a$, T_a -10° and T_a - 20° for an aperture of 45° and no aperture, above black body (BB) and "Ideal" sky emitter surfaces. Ambient temperature is 290 °K (17 °C). Also tabulated are the stagnation or effective sky temperature T_a* and the temperature T_{sx} estimated from equation (6).

Table 2 Estimates of each contribution to reductions in output for non-ideal surfaces and practical set-ups for T_a = 290 K with a 45° aperture. Estimates are to the nearest 5 Wm^{-2}.The partial sum is also used to estimate output when $T_s = T_a$ and removing the mirror term allows estimates of corrections for the case when a heat mirror is not used.

Table 1

Aperture	Type of surface	T_s(°C)	P_{rad} (net) Wm^{-2}	BB/Ideal Cross-over T_{sx}	T_a* (stagnation temperature)
45°	BB	17 7 -3	254 201 154	- 28°C	-47 °C
	"Ideal"	17 7 -3	116 98 81		-119° C
90°	BB	17 7 -3	99 47 0	17°C	-3°C
	"Ideal"	17 7 -3	98 80 62		-72 °C

Table 2

Contribution to output reduction	**Reduction for near "ideal" sky window emitter(Wm^{-2})**	**Reduction for near black body emitter (Wm^{-2})**
Heat mirror (e = 0.1)	20	20
Polymer cover (T = 0.9)	10	20
Absorptance outside sky window (a = 0.1)	-10	N/A
Real surface spectral props.	10	10
Partial sum (~ reduction when $T_a = T_s$)	**30**	**50**
Non-radiative heat gains $T_a - T_s$ =10°C (U =1.5 $Wm^{-2}°C^{-1}$)	15	15
Total correction at	**45**	**65**

$T_a - T_s = 10°C$		

Figure 1.

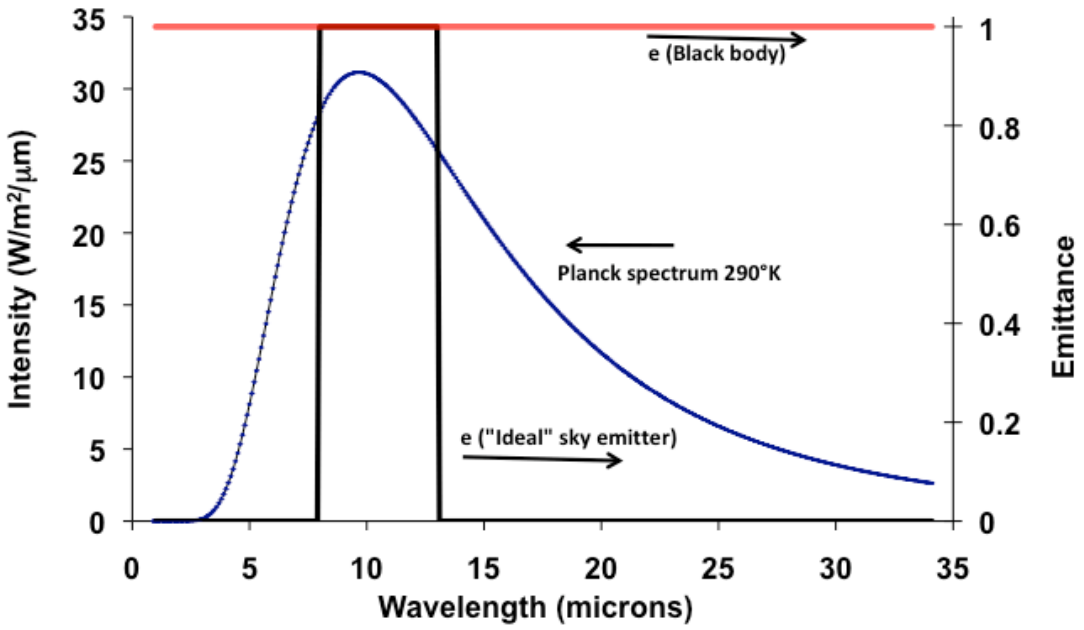

Figure 2.

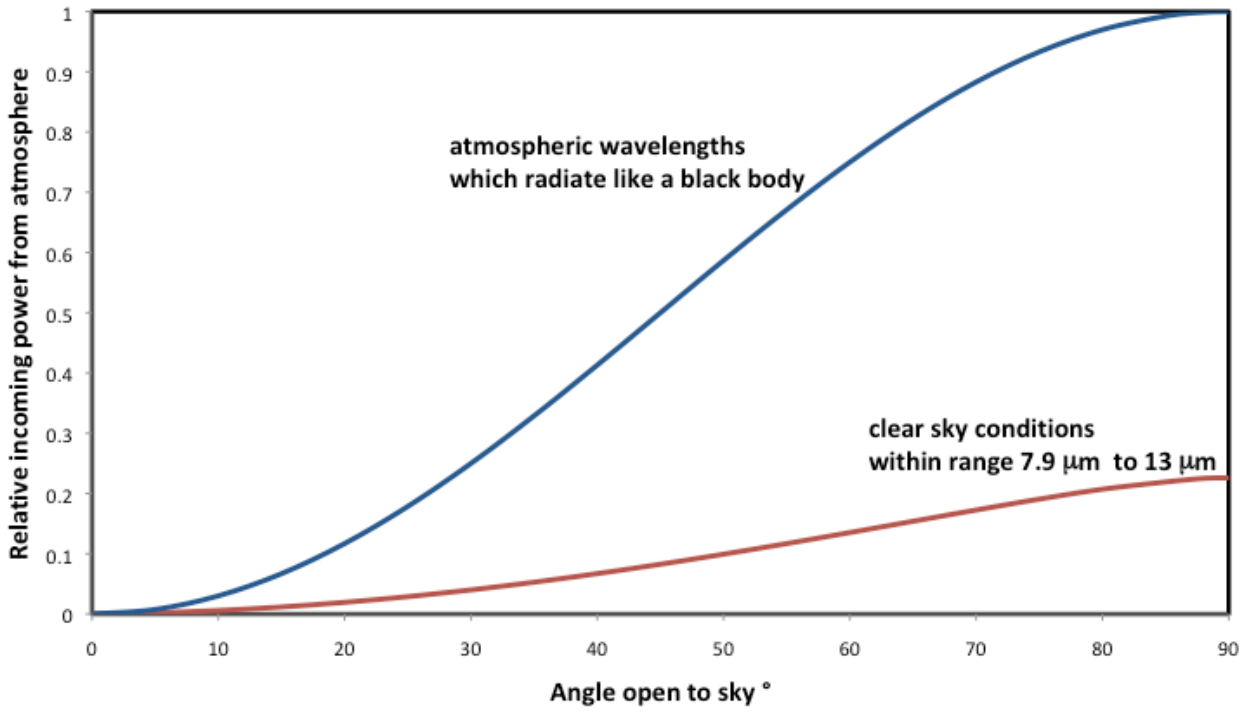
Relative incoming power from atmosphere
1
0.9
0.8
0.7
0.6
0.5
0.4
0.3
0.2
0.1
0
0
10
20
30
40
50
60
70
80
90
Angle open to sky °
atmospheric wavelengths
which radiate like a black body
clear sky conditions
within range 7.9 μm to 13 μm

Figure 3

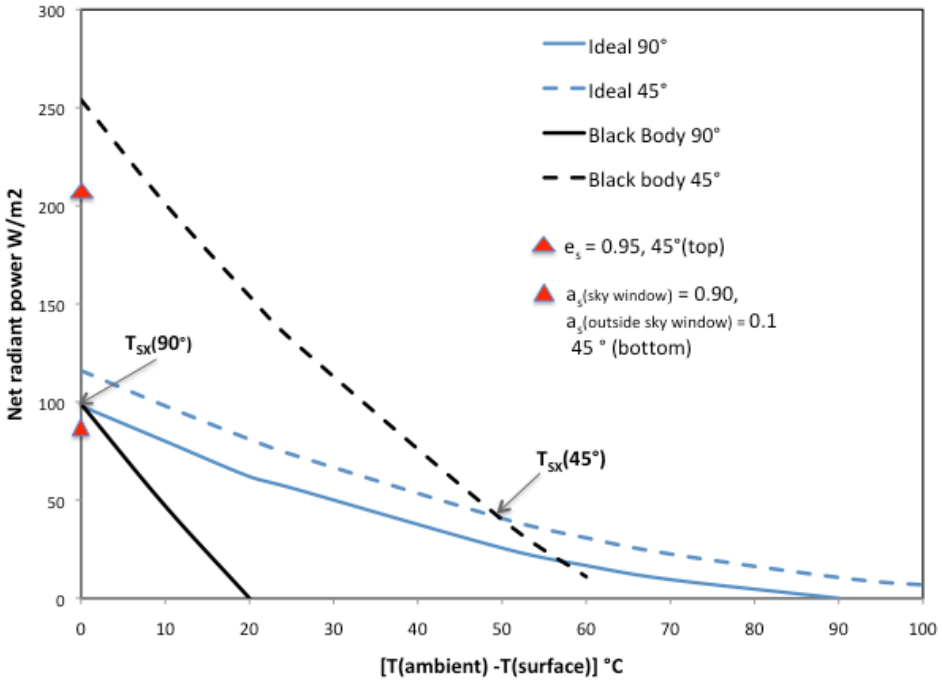
Net radiant power W/m2
300
250
200
150
100
50
0
0
10
20
30
40
50
60
70
80
90
100
[T(ambient) -T(surface)] °C
Ideal 90°
Ideal 45°
Black Body 90°
Black body 45°
e_s = 0.95, 45°(top)
a_s(sky window) = 0.90,
a_s(outside sky window) = 0.1
45 ° (bottom)
T_SX(90°)
T_SX(45°)